MICROSTIMULATORS AND MICROTRANSDUCERS FOR FUNCTIONAL NEUROMUSCULAR STIMULATION

Contract #N01-NS-5-2325
Quarterly Progress Report #2
Period: June 10, 1995 - September 9, 1995

ALFRED E. MANN FOUNDATION FOR SCIENTIFIC RESEARCH
12744 San Fernando Road, Sylmar, CA 91342
Joseph H. Schulman, Ph.D., Principal Investigator
Primož Strojnik, D.Sc.
John Gord, M.Sc.

BIOMEDICAL ENGINEERING UNIT, QUEEN'S UNIVERSITY
Kingston, Ontario K7L 3N6 Canada
Frances J.R. Richmond, Ph.D., Principal Investigator
Gerald E. Loeb, M.D.

PRITZKER INSTITUTE OF MEDICAL ENGINEERING
Illinois Institute of Technology, Chicago, IL 60616
Philip R. Troyk, Ph.D., Principal Investigator

ABSTRACT

During the last Quarter, the focus was on manufacturing of working and hermetically sealed microstimulators both for the needs of Queen's University as well as for the presentation at the 26th NIH meeting in Bethesda in October this year.

The Pritzker Institute has been actively supporting the microstimulator wafer rework and the new package developments.

A short video on microstimulator assembly was produced for presentation at the same occasion. Also, the final seal (the laser weld of the Iridium electrode to platinum/iridium microtube) was developed.

The contribution of the Queen's University for this period is a copy of a paper on micromodular implants, submitted for publication , as an appendix.

INTRODUCTION

We are developing a family of implantable micromodular devices for use in functional electrical stimulation (FES) for various clinical applications, including reanimation of paralyzed limbs.

These devices fall into two categories:

1. Microstimulators that generate precisely metered, highly localized electrical pulses.
2. Microtelemeters that digitize and transmit data from bioelectrical sources and transducers.

Large numbers of these devices can be implanted and controlled by a single, external coil that transmits power and command signals by inductive coupling from a highly efficient power oscillator and modulator circuit in a wearable control box. The devices generally consist of a microcoil wound on a ferrite core, a custom IC chip, and a glass cylindrical capsule (approximately 2 mm diameter by 10 mm long) which may contain glass-to-metal feed-throughs for electrodes at the ends.

This contract is concerned with the further development and in vitro testing of the microstimulator package and specialized electrodes that store energy for stimulus pulses in an electrolytic capacitor consisting of anodized tantalum, activated iridium and the intervening body fluids. It also requires the development of a transducer suitable for sensing the angle of the wrist and the development of a microtelemetry module for outward transmission of this signal.

Work at the Alfred E. Mann Foundation

1. *Further laser development*

To prevent the Ta stem from burning during the exposure to high temperatures, an argon gas dispenser was added to the glass-blowers lathe. The argon spray effectively removes most of the oxygen from the working area which was demonstrated by scorching a wooden stick with the laser without igniting it. Figure 1 shows a tantalum slug with a glass bead sealed to its stem and a Pt/Ir washer laser-welded to the stem.

2. *Videotaping of microstimulator assembly - sealing procedure*

A short videotape was produced for presentation at the annual NIH workshop in Bethesda, MD. It shows all the glass sealing stages in the microstimulator manufacturing including sealing of a glass bead to an tantalum stem, sealing of a glass capillary to this bead, insertion of an electronic assembly and a spring into the capillary and finally sealing of the glass bead with a Pt/Ir μtube to the glass capillary while compressing the spring. The taping was done using a video-camera attached to a microscope.

3. *Electronic assembly, stacked chips, side by side chips*

As reported in the 1st Progress report of this Contract, a plan was developed to rework the microstimulator integrated circuit wafers which had been fabricated at the end of the first microstimulator NIH contract.

That circuit was not fully functional due to problems associated with the on-the-chip demodulation/rectifier diode. In the first manufactured microstimulators, an external diode had been used to bypass the internal diode (Fig. 2-A). Unfortunately, the external diode also bypassed a 500 ohm series resistor needed for proper data demodulation. In later prototypes, a trace connecting the diode and the series resistor was cut with a trimming laser and an external resistor was added (Fig. 2-B). Because the external diode and resistor could accept only the first bond (ball bond), an intermediate land was created that could accept the second bond, (wedge bond), and thus enable the series connection of the diode and the resistor (Fig. 2-C). Even though the scheme worked very well on a bench, these microstimulators failed to work a few weeks after encapsulation. This was probably due to inaccurate laser aim and some other mechanisms such as water vapor ingress into active silicon structures through the damaged passivation layer. Fig. 3 shows the schematic arrangement of the components in the modified microstimulator.

This time we decided to cut the diode trace not with a laser but manually, using an ultrasonic trace cutter and to protect the consequently exposed active silicon. This was done as part of the gold-bump process which includes deposition of a thick layer of nitride over the wafer. The original function of this layer is to insulate the gold traces from the underlaying circuitry, however it can also be used successfully to cover and protect the opening in the original protective layer where the diode trace was cut. It took 50 cutting probe tips and two weeks to cut diode traces on more than 1200 chips on the wafer.

4. *Gold-bump chip*

A wafer with gold-bump chips has been delivered from a vendor for testing. Figure 4 shows a modified chip with gold traces connecting the original bonding pads to new bonding pads on the right side of the chip.

At the Foundation, the wafer was 100% electrically tested and the bad chips were marked on the wafer with indelible ink. Electrical testing revealed that there were 1003 good chips and 136 bad chips on the wafer, which represents a 88% yield.

Before the diode trace cutting at IIT, this wafer had been visually inspected for physical damages and the chips identified as bad were marked on a wafer map. A similar wafer map was also made at the Foundation after the electrical testing showing the bad chips. The two maps, showing the wafer before and after gold-bump processing are shown in Fig. 5. It can be observed that the gold-bumping process did not significantly increase the number of bad chips.

Transposition of bonding pads using a gold-bump process enabled us to use the previously designed and manufactured Microprinted Circuit Board μPCB as the μstim chip substrate. A problem arose, however, because on the μPCB there was space provided only for an external diode and not for an external resistor. A solution suggested by an outside vendor was to use a chip resistor with a conductive back which serves as an electrical contact and mount it atop the rectifying diode thus making a series connection to the diode. The diode would then be placed on its designed position and the wire-bond previously designed to make connection to the diode, would make connection to the chip

resistor. This scheme did not work due to conductive epoxy spill-over resulting in several electrical shorts.

The second solution was to reassign the conducive areas on the μPC Board and to place the chip resistor and the diode each on a separate conductive pad. This version has a serious disadvantage, namely a long bond wire going from the Coil High pad on the chip to the Coil High conductive area on the μPC board. To stabilize this and other bond wires a glob top epoxy has to be applied over the exposed chip and bond wire area. The original and the modified component arrangements are shown in Figs. 6-A and 6-B.

5. *Helium leak testing*

A more sensitive helium leak tester has been acquired by the Foundation. This leak tester allows detection of leaks as low as 5×10^{-11} atm-cm^3/s and displays the result on an analog meter.

Laser welded test seals have been made between Ta wire and glass beads that had no detectable leak when measured on this tester. However, when verifying the results with another, digital leak testing machine, leakages in the order of 2×10^{-10} atm-cm^3/s were detected. We are still trying to find an explanation for this discrepancy in results.

6. *Microstimulator production*

Before the NIH meeting this year, we were able to build the first hermetically sealed microstimulator using the new assembly procedure, shown in Figure 7. New YAG laser-

welding protocols were developed that make possible welding of Pt/Ir washers to Pt/Ir μtubes without closing the lumen of the tube. The main problem was the size of the YAG laser beam. The beam diameter at the focal plane is 8 mils while the size of the μtube is only 5 mils. Special jigging, miniature heat-sinks and beam intensity modulation were required to make a successful weld.. The same laser was used to make the final seal that welds the iridium washer to the platinum/iridium μtube and seals off the μtube. Figure 8 shows the final seal. Four laser welding marks can be clearly seen on the Ir electrode.

7. *Contact spring*

The first batch of springs that by compression force enable electrical contact between the electronic assembly and the electrodes contact were slightly too large for proper installation within the glass capsule. New springs were delivered and consequently gold-plated. The dimensions appear to be right. Force measurements were performed on a 20 unit sample. The springs were compressed to one half of the original length, which is approximately what happens in μstim production. The average force was 0.56 newton (56 grams), the maximum and minimum force were 0.52 N and 0.65 N respectively. With the weight of the electronic assembly being under 0.05 gram, the axial acceleration required to break the connection between the assembly and the electrodes must be 11200 ms^{-2} or 1120 g.

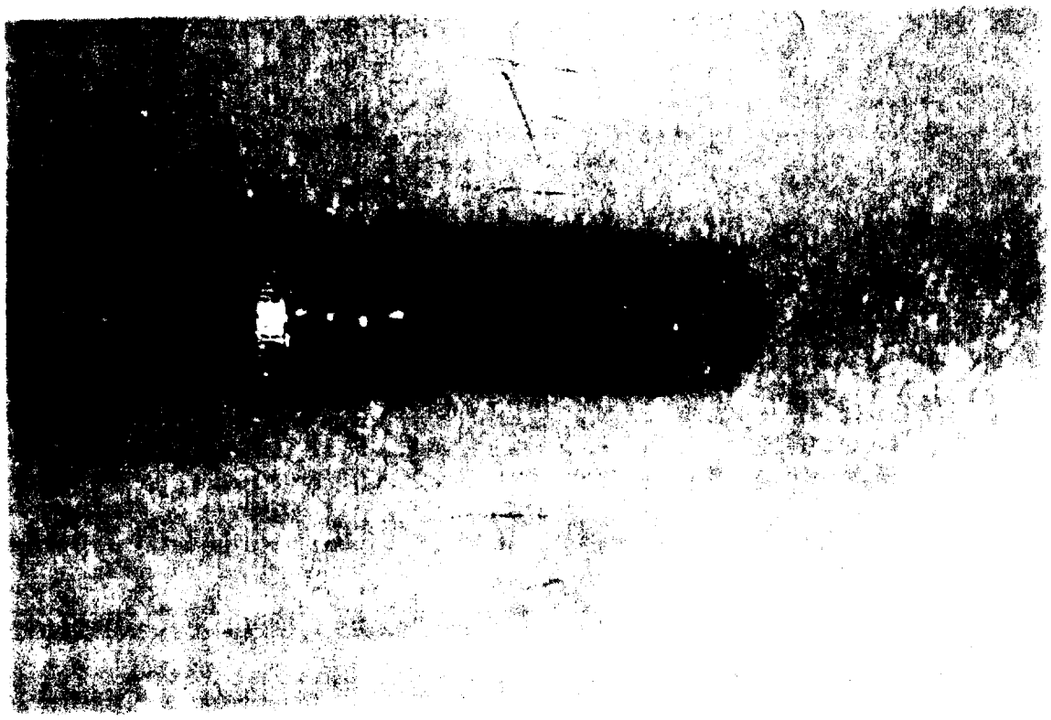

Fig. 1

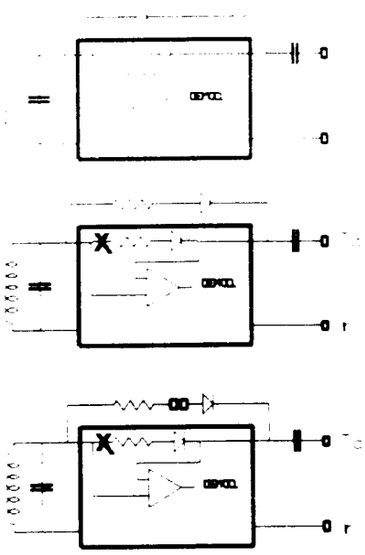

Fig. 2

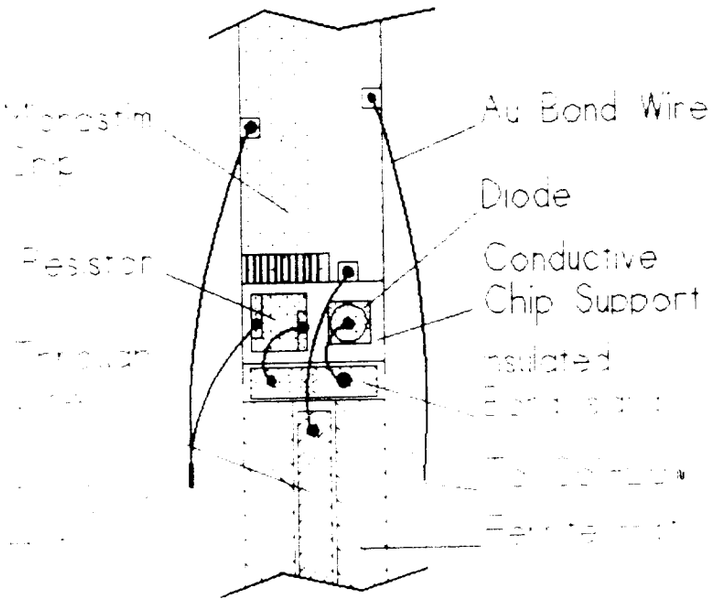

Fig. 3

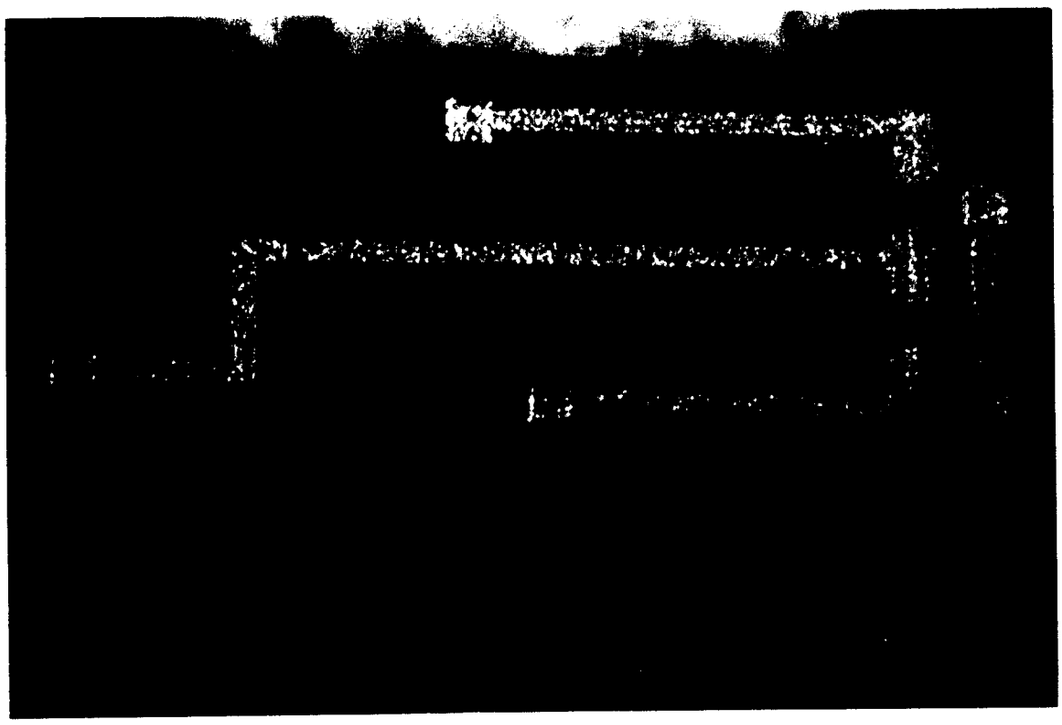

Fig. 4

Fig. 5

Fig. 6

A

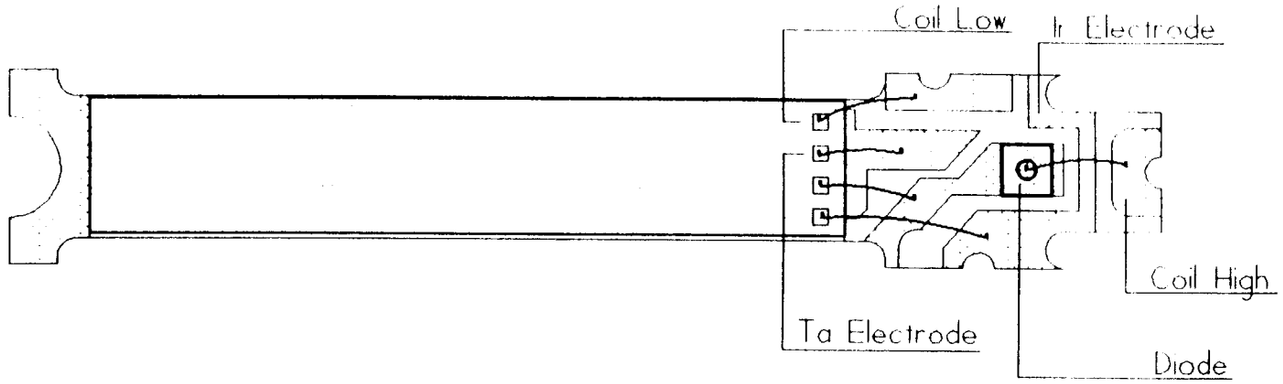
Coil Low
Ir Electrode
Coil High
Ta Electrode
Diode

B

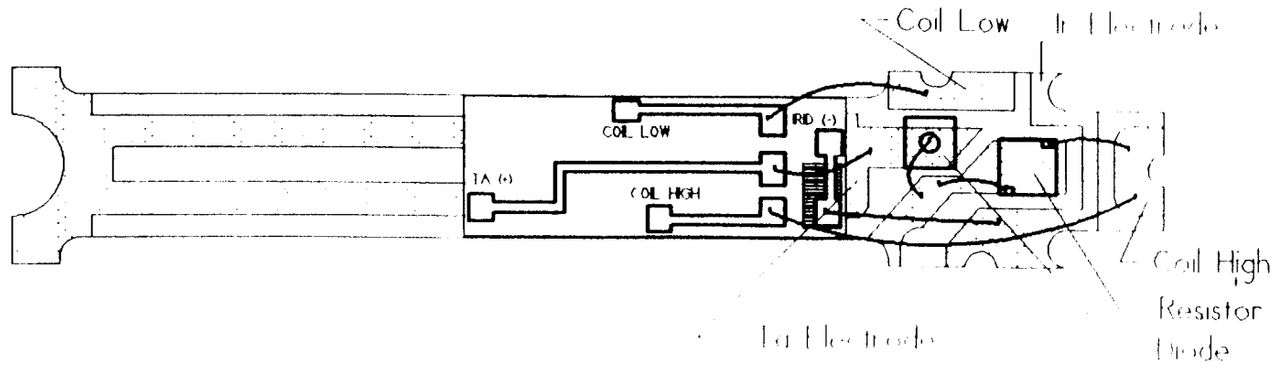
Coil Low
COIL LOW
RD (-)
TA (+)
COIL HIGH
Coil High
Resistor
Diode

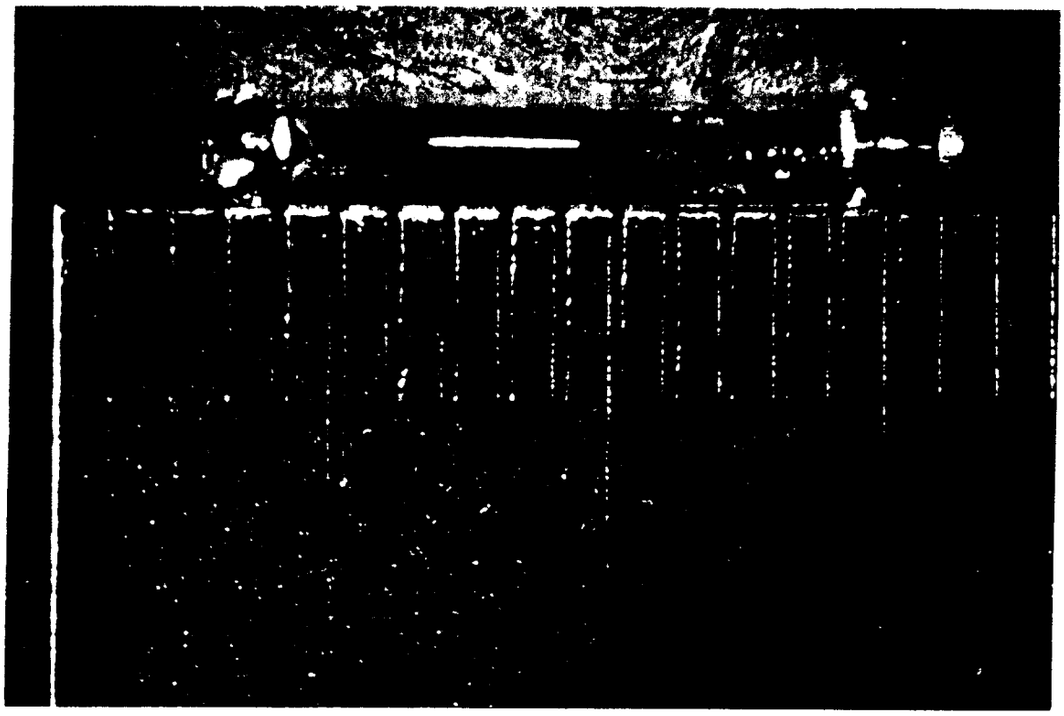

Fig. 7

Fig. 8

September 19, 1995

Micromodular Implants to Provide Electrical Stimulation of Paralyzed Muscles and Limbs

T.Cameron, G.E Loeb, R.A.Peck,

J.H.Schulman*, P.Strojnik*, and P.R.Troyk**

Queen's University, Kingston, Ontario; *A.E. Mann Foundation for Scientific Research, Sylmar, California; and **Illinois Institute for Technology, Chicago, Illinois

Tracy Cameron, at Queen's University, Biomedical Engineering Unit, Abramsky Hall, Kingston, Ontario, K7L 3N6; phone (613) 545-2790; FAX (613) 545-6802; e-mail tracy@biomed.queensu.ca

10

Introduction

Therapeutic electrical stimulation (TES) can strengthen muscles paralyzed from upper motor injury or disease [1] [2] or those that have atrophied from inactivity following surgery or trauma [3][4][5]. Functional neuromuscular stimulation (FNS) has provided individuals with the ability to initiate movements that are of functional value, such as the restoration of limited grasping functions after cervical spinal cord injury [6][7][8][9] and the restoration of ambulation by FNS alone [10][11] or in combination with orthotics [12][13][14]. FNS has also been used to improve ventilation by stimulation of the phrenic nerve [15][16], improve bladder, bowel and sexual function by stimulation of the sacral anterior nerve roots [17][18][19][20], and reduce spasticity [21][22].

Two main interface techniques have been used in the application of FNS to paralyzed muscle. The first involves the surgical implantation of electrodes directly in or on muscles and nerves. This has been accomplished by using fully implanted multichannel systems that require long wire leads to connect to remote electrodes. These systems are cumbersome to implant and prone to mechanical failure. Percutaneous wires implanted into muscles have also been used but pose unacceptable problems of cosmesis, maintenance and infection. The second strategy has been to apply surface electrodes to the skin over the muscles of interest, but the recruitment of individual muscles is not sufficiently selective for applications requiring fine control of motion. These electrodes can also be difficult to don and maintain and may produce skin irritation and unpleasant sensations related to activation of cutaneous nerves. Several groups of researchers have attempted to solve some of these problems by designing single channel implantable stimulators. These miniaturized stimulators can be located at or near their individual targets [23][24]. These devices, though fairly small, were of limited use because they did not provide the stimulus control and multichannel addressability needed for most motor tasks.

We are developing a family of implantable electronic modules that can be used in a variety of combinations to stimulate individual nerves and muscles (uStim) or to measure and transmit information from the limb to the external controller. These modules eliminate the donning and reliability problems of surface and percutaneous electrodes and do not require long leads between the electrodes and the controller, as data and power are transmitted by RF signals. Their small size allows injection directly into the desired muscles through a hypodermic needle, providing virtually unlimited numbers of highly selective channels without requiring surgery.

Technical requirements

Requirements	Implementation
minimal surgery	small size allows injection into muscle through hypodermic needle
custom configuration	multiple single channel stimulators can be combined in an unlimited manner
avoid lead breakage	wireless transmission of data and power
long life	hermetic package, no batteries
safe	capacitive charge storage, charge balanced output stimulation
precise	digitally controlled stimulating current amplitude and duration
stable tissue interface	package designed for tissue fixation without progressive encapsulation

Design

Specifications

a) size 2 mm diameter, 13 mm length

b) packaging: glass encapsulated

c) power: inductive coupling from an external coil (2 MHz)

d) physical range: anywhere within a cylindrical coil or one radius from the face of a flat coil

e) number of unique addresses: 256

f) pulse width control: 3-258 μsec, 1 μsec steps

g) pulse amplitude control: 0.2 to 30 mA in two ranges of 15 linear steps each (0.2 and 2 mA, respectively)

h) pulse waveform: monophasic square with capacitive coupling for charge balancing between pulses

i) waveform options: two recharge current settings, 20 or 200 μA. two pulse shapes, square or exponential tail.

Package design considerations

The main distinguishing features of the μStim are that multiple stimulators can be implanted allowing for the control of an unlimited number of highly selective channels, without requiring surgery, and without compromising the integrity of body tissues.

The first feature restricts the size and shape of the device to a cylindrical capsule (Figure 1) that can be injected into a muscle through a 12 gauge hypodermic needle. The second feature concerns the control of multiple implants. Each device must be uniquely addressable and capable of delivering a variety of pulse durations and intensities. Addressability and digital control of stimulus pulses are accomplished by the implementation of electronics within the device. The third feature requires that internal components of the stimulator be electronically

isolated from the body fluids, and that leads between the controller and the stimulator power and data be eliminated in favour of RF transmission.

Biocompatible borosilicate glass was used to encapsulate the internal components hermetically while adhering to the constraints on package size and electromagnetic transmission. Sintered Tantalum (Ta) was used as one electrode material because it is able to act as a 'capacitor-electrode' with respect to body fluids. In this application, the stimulus charge must be stored on the electrode material itself because the limited size of the device does not allow for the inclusion of an internal storage capacitor. Iridium (Ir) was chosen as the other electrode material because of its nonpolarizing low impedance interface. This combination of tantalum and iridium has been found to perform well during extensive electrochemical testing [25].

Ir activation was required in order to lower the interface impedance. However, Ir activation could not survive the heat required to fuse the Ir ball to the glass capillary. Similarly, sintered Ta is somewhat fragile and can be damaged or contaminated during the assembly process. Electrochemical conditioning of both the Ir and Ta electrodes were therefore carried out after the capsule was sealed as described by [25].

Tantalum electrode

The sintered anodized Ta slug used in the μStim stores charge by acting as a 'capacitor-electrode' with respect to the body fluids [26]. Loosely packed tantalum powder was sintered-on the end of a solid Ta wire (0.25 mm Dia.) to form a porous tantalum cylinder (slug) many times increasing its available surface area (geometric surface area 9.60 mm^2). The anodization of tantalum forms a dielectric of tantalum pentoxide whose thickness is proportional to the anodization voltage (20 A per volt)[26]. Working μStims were anodized by applying a limited current of 0.1mA with a compliance of 37 Volt and holding for one hour longer than required to reach the compliance limit. Anodization current was applied by probing the iridium contact and passing the current through the circuitry and out the tantalum electrode, which was immersed in 0.1% phosphoric acid solution.

Iridium electrode

This electrode was polarized cathodically with respect to tantalum. Iridium is an excellent electrode material as it can be electrochemically activated using cyclic voltammetry [27] dramatically increasing its charge injection limit. The multilayer oxide film formed on Ir by repetitive potential cycling may produce as much as a 100-fold increase in the charge capacity of the surface [28]

$$Ir^{+3}(OH)_3 + H_2O \Leftrightarrow Ir^{+4}(OH)_4 + H^+ + e^-$$
$$Ir^{+3}(OH)_3 + OH^- \Leftrightarrow Ir^{+4}(OH)_4 + e^-$$

Activation was accomplished by touching an iridium probe wire to the electrode surface. Although this procedure results in an area of incomplete activation at the contact point between probe wire and electrode surface, the electrochemical properties of incomplete Ir coatings are known to be dominated by the activated region. Iridium was activated by repetitive cycling at 500 mV/sec between -0.64 V saturated calomel electrode (SCE) and 0.86 V SCE in phosphate buffered saline (PBS). The current between the Ir electrode and the reference electrode was plotted as a function of potential (E) on an X-Y recorder (Figure 2). The charge capacity after 1 hour of activation increased from a pre-activation capacity of 1.2 mC/cm^2 to 15.6 mC/cm^2.

Hermetic seals

μStims were hermetically sealed in N51A borosilicate glass. Such glass is an excellent material for this use as it is extremely biocompatible [29] and it is stable at neutral pH, so it is able to maintain hermeticity between body fluids and the electronic circuitry for extended periods of time. Another important reason for using glass is that it can be melted to form seals to other oxide surfaces such as on most metals. Three such seals are needed in the

fabrication of the μStim; glass-to-Ta, glass-to-Ir, and glass-to-glass. Glass-to-metal seals must pass helium leak tests of detection limit $1 \times 10^{-10} cm^3 s^{-1}$ atmosphere^{-1}. The small size of the μStim makes it extremely sensitive to any water that is trapped in the package at the time of sealing or leaks into the package that may occur later. The amount of water vapor that would pass through a leak just below our sensitivity limit would reach saturation in about 200 days. We are planning to include a small crystal of the water getter colbalt chroide. This will greatly increase the time it will take for water to saturate even with a leak below our detection limit. These glass to metal seals have been previously tested and the results are discussed in [25]. Many of the problems in making glass-to-glass and glass-to-metal seals have been well-studied by the electronics industry, which has been using glass encapsulation techniques for many years in the fabrication of relays and diodes.

Stresses created during sealing can lead to cracks and these cracks are accelerated by scratches or abrasions on the glass, particularly in a polar liquid such as water [30]. Quantitative analysis of the stress in low and high stress devices is shown in Figure 4. A quarter-wave filter was inserted into a polarimeter converting the light to a monochromatic state. By rotating the cross-polaroid either clockwise (cw) or counterclockwise (ccw) nulls are attained in regions of stress. These regions are marked by the arrows in Figure 3, and are barely visible in the low-stress seals. The mean angular rotation and the cylindrical geometrical factors are used to compute tensile stress in pounds per square inch (psi) in these regions as shown in the equation in Figure 3. After examination of the various seals it was determined that stresses were created by an uneven distribution of heat during seal formation which was exaggerated by the use of heat sinks. Mock-ups fabricated by rotating the device at 78 rpm and removing all heat sinks, with the exception of the Ta heat sink, exhibited the least amount of stress and most uniform annealing. The Ta heat sink acts to protect the Ta slug from possible ignition during sealing as well as holds the device in place. The stresses in these samples were consistently under 2,000 P.S.I., with evenly distributed compression on

the metal feedthroughs as desired to maintain hermeticity. Thus all subsequent μStims were sealed under these conditions.

Fabrication sequence

The μStim is fabricated in three main steps. The first step involves preparing the electrodes. A glass bead is melted to each electrode stem in preparation for encapsulation in the glass capillary tube at a later step. This is necessary to protect the IC chip, which would be damaged by the heat conducted from the glass-to-metal sedaling, whereas the lesser heat conducted during the glass-to-glass sealing is safe for the chip. The second step involves assembling the various internal components (listed in Table 2) and attaching them to the Ta-glass bead end, and attaching the glass capillary to the Ir-glass washer end. The final step involves inserting the assembly into the Ir-glass capillary section and making a final hermetic seal at the Ta-glass bead to glass capillary junction. Figure 4 shows the various components and their relationship to each other. The three steps are described in more detail below.

The Ta stem is first polished (by hand using a miniature rotary polishing tool and a polishing paste containing diamond dust) to remove any longitudinal grooves formed during the drawing of the wire by the manufacturer. Such features interfere with the ability to achieve a completely hermetic seal. The stem is then cleaned in petroleum ether, followed by alcohol, and finally distilled water. The Ta slug is then inserted into a Ta heat sink/holder and a microtorch used to melt a glass bead onto the Ta stem. Ta is used for the holder in order to reduce possible contamination of the electrode by foreign metals, which would interfere with later anodization. The microtorch uses a pressurized natural gas and oxygen flame and the torch tip utilizes a 22 gauge blunt tip disposable needle[6]. The end of the stem opposite the Ta slug is ground flat and cut to length, providing a surface for spot-welding in a later step. The Ir electrodes are manufactured by melting a piece of iridium wire .010 " in diameter to form a ball of approximately .065" in diameter. A glass washer is then melted onto the stem and back side of the ball and the stem cut to length (Figure 4B).

The second step begins by heat-sealing the Ir ball-glass washer assembly to the glass capillary and cutting the capillary to length. The Ir ball on the Ir-capillary assembly is polished and cleaned, as described for the Ta stem, and put aside to be used at a later step. The main step in the assembly of the internal components is to mechanically connect the two electrodes and the copper coil to the integrated circuit (IC) chip. This begins by using epoxy to glue a metal shim to the bottom half of the ferrite core. The shim serves as a platform for the IC chip and diode. The Ta-glass bead assembly is then spot welded (20 Ws) to the shim. A gold-plated wire feed-through is glued into the groove of the ferrite bottom, for later use as a contact between the IC chip and the Ir ball electrode. Next, the IC chip and diode are attached to the metal shim with conductive epoxy, and connections between the electrodes and chip are made using a wire ball bonder on the chip surface and conductive epoxy on the metal shim and feedthrough surface. Hanging gold wires are then bonded to the IC chip to provide a means of connecting the coil wires. The ferrite top is bonded to the ferrite bottom with cyano acetate and the copper coil wound around the entire core. The self-resonance frequency of the coil is adjusted to be 2 MHz (± 0.025%). Next, the free ends of the coil leads are stripped of their insulation and attached to the hanging gold wires with conductive epoxy.

In the final step conductive epoxy is inserted into the Ir-glass capillary assembly to provide an electrical connection between the Ir ball and the IC chip (via the gold plated feed through wire inside the ferrite core). The rest of the assembly is then inserted into the glass capillary. Finally, the glass bead at the Ta end is fused to the glass capillary, hermetically sealing the internal components of the device.

µStim Control

Power transmission

Magnetic inductive coupling is used to transfer power and data to the implanted devices. The main problem with this type of transmission is that it relies on an airgap transformer that has a very low coupling coefficient between the primary and secondary windings. A carrier at

2 MHz was chosen for this application because it lies between the AM and FM radio bands it can be easily divided into a 1 μsec clock needed for pulse width control, it can be handled efficiently by CMOS circuitry, and it allows sufficient Q to be obtained between the transmitting coil and the small self-tuned receiver coil. Details of the class E driver used to obtain efficient power transmission from the external controller to the implanted μStim are described in [31][32]

Data encoding

A single stimulus pulse from a single μStim is specified by three 8-bit command words [25]. A 2 MHz carrier is amplitude modulated to transmit this information. Manchester encoding was used because it requires at leact one state change every bit, thereby insuring a constant load to the transmitter. A zero is encoded by maintaining state during the bit (8 cycles (8 μs)), and a one is encoded by a state change after the 8th cycle (4 μs). A low state is 80% of the high state in carrier amplitude. A complete transmission requires 288 μs, enabling a possible 69 separate devices to be activated in a sequence at the maximum specified rate of 50 Hz for each device. During the idle period between commands, alternating zeros and ones are transmitted to all implanted devices. The beginning of a command is signaled by transmitting a ready code made up of five 0 bits. This code is followed by three command words which code for the μStim address, pulse width, and waveform.

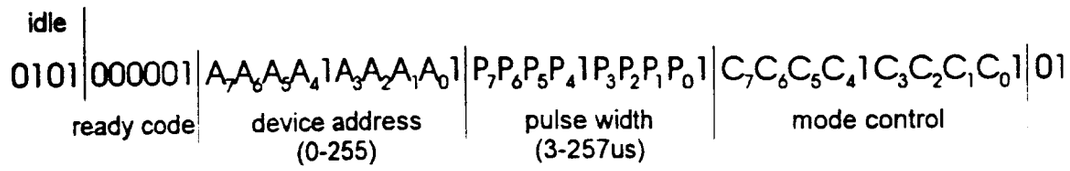

Each μStim contains an 8-bit address stored in its read-only-memory, which it compares to the address sent by the controller. If a match is found, the remaining two command words are

decoded to determine the pulse width, current, recharge rate, and shape. The second 8-bit word decodes the pulse width, which varies from 3 to 258 μsec in 1 μsec steps (a minimum of 3 μsec occurs due to the finite time needed to switch the circuitry). The final 8-bit word determines the rest of the stimulus parameters. The four high bits (C_7--C_4) are used for the stimulus current amplitude, providing 16 levels. Bit 3 determines the current range, low (0 to 3 mA, .2mA steps) or high (0 to 30 mA, 2 mA steps). Bit 2 determines the pulse shape, which can be square or have a tail that drops exponentially. A stimulus waveform that has an exponential tail can be used with certain nerve cuff electrode configurations to preferentially stimulate small diameter motor axons while anodally blocking large axons [33]. Bit 1 selects the recharge current (20 or 200 μA), and bit 0 is used to maintain even parity, which is used as one of the data integrity checks by the μStim. An additional check consists of the mandatory data=1 bits that occur every fifth bit, these also assure that the five sequential zeros used as the ready code are unique.

External control

External control of the μStims was accomplished by a Motorola 68HC11 microcontroller connected to an Actel A1020 series field programmable gate array (FPGA) [34]. This architecture was chosen for its flexibility and small size. The Motorola 68HC11 contains the required ports and ample memory on a single chip so as not to require further hardware. This hardware was programmed as a stand-alone device to deliver stored stimulation sequences at regular intervals. During the chronic animal experiments, information on up to four cats was programmed into the internal memory (EEPROM) and used to produce the desired stimulation sequences for the training sessions. A second program allowed the real time control of the implanted μStims. In this mode, the pulse width and waveform controls were set by adjusting dials on the front panel of the control box. Both modes controlled up to four different μStims. When instructed, the three 8 bit control words were sent sequentially to an 8 bit parallel port on the FPGA. The FPGA performed a parallel to serial conversion, adding the

various additional bits required by the transmission protocol and the Manchester encoding needed by the carrier modulating circuitry. The digital circuitry was implemented on an FPGA in order to reduce the physical size of the control unit while maintaining flexibility during the design and testing phase

Test methods and results

In vitro Testing

μStims were tested in saline filled test wells (20 mm x 4 mm x 6 mm), each containing non-contacting pickup electrodes. The stimulus current generated potential gradients in the saline bath that were recorded differentially by the recording electrodes. This signal was then displayed on an oscilloscope screen and measured. The output voltages were found to be linear over the low (standard error of estimate (Sy.x) = 0.006973) and high (standard error of estimate (Sy.x) = 0.031454) current range, up to the compliance voltage limit of the device in the bath. The impedance of the bath was calculated to be 500 Ω (Figure 6). A second test bath was built to provide precise and accurate measurements of stimulus and recharge currents and compliance voltages produced by the μStims. It is analogous to the sucrose gap technique used to monitor the action currents produced by an axon, which involves forcing the currents through an external path whose electrical resistance can be controlled. Using this technique, a compliance voltage of approximately 8.8 V was calculated. The two recharge current rates were measured to be 20 μA and 200 μA, respectively. A measurement of the output voltage when the devices were commanded to produce maximum currents (30 mA) with maximum duration pulses (255 μsec), and varying interval rate is shown in Figure 7. As the rate was increased above the interval needed to fully recharge the capacitor electrode, a steady decline in output signal occurred. The 3 dB cut off frequency was found to be 15 Hz at a the 20 μA recharge rate and 120 Hz for the 200 μA recharge rate. The devices were also tested for their sensitivity to orientation inside the coil. The mean angular deviation from the

center line up to the limit of where the μStims functioned normally was found to be ± 55.5 ± 6.4 degrees (n = 10)

In vivo Testing

Sixteen devices were implanted into the hindlimb muscles of 4 cats. These devices were activated 2 hours daily, five days a week for a period of up to 3 months [34]. These devices were examined before and after implantation by dissecting microscope and environmental scanning electron microscope (ESEM; Model E-3, Electroscan) inspection. Post-implant ESEM views of both electrode surfaces showed no detectable changes from non-implanted electrodes except for a dense coating of connective tissue on the corners of the tantalum slug (Figure 8). μStims were also tested for leakage currents before and after chronic implantation into the hindlimb muscles of a cat. These curves were found to be essentially identical between the pre and post-implants states (Figure 9). At a nominal operating level of +10 VDC, leakage currents were measured as 6μA (preop) and 1μA (post-explant). The difference between these values is probably attributable to differences in the settling time used between setting the voltage and measuring the current. Sintered anodized Ta in saline acts like an RC circuit with a long time constant, particularly for the deepest pores of the structure. A post-implant DC capacitance was estimated to be 2.7 μF, which is consistent with the value expected for the thickness of the anodization layer.

Failure Modes

Gross Leaks

These leaks resulted in visible water condensation on the glass walls within a few hours to a few days of in vitro testing. They were associated with visible cracks in the seals, apparently due to stresses in the glass. The incidence of such cracks was reduced after the changes in

sealing procedure described above, but yields remained low (about 40%). The sealing protocol for future devices has been further modified to address this problem [35]. Future devices will use a glass feed-through composed of a small Pt/Ir tube. This tube will allow the hot expanding air inside the capsule to escape. It will also allow any moisture and residual gases to escape during the final unit bake-out. The final seal of the uStim capsule will be performed by laser-beam welding. This method of sealing will reduce the stresses on the glass by focusing the heat. An iridium disk electrode will be laser-welded to the tube after bake-out, forming the final hermetic seal in an inert atmosphere.

Entrapped Water Vapor

The current microtorch sealing method and the various hygroscopic internal components made it impossible to totally eliminate water vapor trapped within a hermetically sealed package. This entrapped water vapor can cause detuning of the coil and subsequent intermittent behaviour. Future efforts will work to eliminate most of the polymeric materials and seal the devices in an inert atmosphere (probably helium, which would facilitate detection of occult fine leaks whose frequency is still uncertain).

Output Connection Failures

The silver-epoxy which connects the electronic components to the iridium electrode stem has tended to become brittle with age. It has also been found to produce undesirable volatiles. This breakage in electrical connection can be detected during a leakage test, which required passage of current from a probe on the external iridium ball though the electronics and out the tantalum electrode into a saline bath. Future effort will to eliminate the use of silver epoxy by including a spring contact.

Summary and Clinical Applications

A single channel implantable electrical stimulator was designed and tested. The μStim devices were found to maintain hermeticity in at least some cases for the duration of the test period (3 months) and were able to produce highly controllable stimulation pulses capable of causing reproducible twitches when applied to various muscles of a cat. This device has many advantages over previous devices. First, it is completely self-contained which eliminates the need for cables and wires that have been found to break over time [36]. The modularity of the device enables it to be easily configured into a custom multichannel system. The use of capacitor electrodes reduces the possibility of a net DC current flow in the event of failure in the control electronics. Anodized Ta has a very low leakage current which was found to be stable or even decrease with chronic stimulation.

The small size and flexibility of the μStim make it an ideal candidate for many FNS application. Multiple μStims can be injected into various muscles or regions of a single muscle allowing for a more precise control of movement without the need for multiple leads and controllers. Eight channel implantable stimulators have been described [37][38][39] with some recent work being done on 30 and 64 channel systems [40]. Control of the μStim can be achieved in any combination of channels from 1 to 256. Its small size also allows it to be easily implanted into locations that may be difficult to reach using standard surgical techniques and electrodes requiring connecting leads. Some of the application of FNS that may be suited for this type of technology include: urinary control, bowel management, sexual function, pain management, as well as the control of manipulation and mobility. Like most FNS approaches, ustims are intended to stimulate muscle contractions secondarily by exciting the terminal branches of motoneurons, so they are most appropriate for paralysis and paresis caused by upper motor lesions in which the motoneurons and peripheral nerves remain intact.

FNS has also been applied to exercise and muscle conditioning. Muscles made inactive by surgery or injury may atrophy [41][42][43]. Reduction in the size and strength of atrophied muscle fibers can be reversed with therapeutic electrical stimulation (TES)

[3][4][5]. The usual method is to apply high levels of current through skin-surface electrodes in order to activate underlying muscle nerves (using an external stimulus generator). However, stimulating electrodes are difficult to don, and may produce skin irritation and unpleasant sensations related to activation of cutaneous nerves. Exercise using FNS has generally been confined to the rehabilitation of SCI individuals by lower extremity cycle ergometry. Along with the obvious muscle hypertrophy (increase vascularity and mitochondrial activity, switch to type I (slow) fibers), it has been found to have positive effects on cardiovascular capacity [44] and bone density [2][45], and reductions in complications such as deep vein thrombosis and dicupiti ulcers. Electrical stimulation has also been found to prevent secondary complications which arise due to neuromuscular damage [46]. Muscle conditioning using FNS has been applied to the reduction of shoulder subluxation in individuals where muscles supporting the glenohumeral joint have become paralyzed [47]. Several groups have shown that by applying surface stimulation to the shoulder region a significant improvement in relaxed shoulder alignment can occur [48][49] Reducing shoulder subluxation by FNS is preferable to the use of slings and supports as they reduce mobility and can lead to the development of capsular adhesions [47]. This improvement can occur in a relatively short period (4 to 6 weeks) however some subjects may require longer interventions. Implanted stimulators could provide a more controlled and precise stimulation and because of their ease of use could used in an outpatient rehabilitation program.

In these particular application FNS has been confined to large muscle groups easily stimulated by surface electrodes. Because of their small size and easy implementation μStims could be used in those muscle located more deeply. They also allow FNS to be applied to the more general population such as those patients undergoing hip or knee surgery. A lack of mobility in these patients can greatly increase there rehabilitation time; by maintaining muscle strength, their recovery time could be reduced. μStims are ideal solutions for these types of FNS applications because they are easily implanted nonsurgically and do not need to be

removed after the rehabilitation period because they are essentially inert when not actively powered.

Conclusions

The μStims described in this paper are electronic devices that can be injected into muscles to exercise and strengthen them (e g. following a stroke or arthroplastic surgery) or to produce movements of functional value, such as grasping and walking. Further testing of this device is presently under way. These tests involve examination of the biocompatiblity of the μStims and their components by implantation and chronic stimulation of these devices in various hindlimb muscles of cats. Glycogen-depletion experiments are also underway in order to assess the distribution of fiber activation within a muscle

Figure Legend

Figure 1 μStim. features L to R anodized Ta-slug, hermetic seal to glass bead and glass capillary walls. Ta stem welded to gold plated metal shim. IC chip with Au wirebonds to copper coil. Ag-epoxy junctions to Cu coil windings over hollow ferrite core. Ag-epoxy connection to Ir ball sealed to glass capillary wall, activated Ir surface

Figure 2. Iridium activation curve measuring the current between an Ir electrode and reference electrode (saturated calomel electrode, SCE) plotted as a function of potential (E) Ir was activated by repetitive cycling at 500 nV/sec, of potential between -0.64 V SCE and 0.86 V SCE in phospate buffered saline (PBS)

Figure 3 Photograph showing regions of high and low stress (arrows) determined by observing the devices under polarized light and examining for nulls (shown by dark regions) Quantitative results for the stresses were made by applying the various values to the formula shown below the photograph. Stress measurements below 2000 psi wre condsidered acceptable for these devices

Figure 4. Exploding diagram showing the various parts of the MicroStimulator and how they are assembled. A: Shows the Ta assembly which is made up of the Ta slug and stem welded to a glass bead. B: Shows the Ir-capillary assembly which is made up of the Ir ball welded to a galss washer sealed to a glass capillary tube.

Figure 5. Diagram of the μStim fabrication sequence showing the various steps involved in the assembly of a μStim. The Ta end and the Ir are made separately with all the internal components being attached at the Ta end first. The final step involves inserting the Ta end and all the various components into the Ir end which contains the glass capillary tube used as the

encapsulating material. Electrochemical conditioning of the two electrodes takes place after the device has been assembled

Figure 6 Graph of pulse amplitude setting versus normalized output voltage. The linear portion of the curves were fitted to straight lines which are displayed on the graph as dashed lines. These lines were found to fit very closely t the data with Sy x values of 7.0×10^{-3} and 3.1×10^{-2} for the low and high current ranges, respectively

Figure 7. Graph fo the frequency of stimulation versus the output voltage shown as a percentage of maximum voltage for the two recharge current rates. The 3 dB cut off frequencies at the two rats are shown by the dotted lines. 15 and 120 Hz for a rate of 20 and 200 μA respectively. Devices were commanded to produce maximum currents and pulse widths throughout this test.

Figure 8. Photograph of environmental scanning electron micrographs of the Ta stem and slug before (pre-op) and after (post-op) chronic implantation. The pre-op scan is shown at a magnification of 270 times and the post-op is shown at 210 times. A layer of connective tissue is seen around the stem of the post-op device.

Figure 9. Graph of the applied voltage versus the measured leakage current for devices before and after chronic implantation into the muscle of a cat. The dotted lines indicate the leakage current measured at the normal operating voltage of 10 V. The leakage current was seen to decrease after chronic stimulaiton within an animal.

References

[1] R.M. Glaser, "Functional neuromuscular stimulation exercise conditioning of spinal cord injured patients," *International J. Sports Med.* vol 15, pp. 142-148, 1994

[2] R.D. Malagodi, M.W. Ferguson-Pell, R.D. Masiello, "A functional electrical stimulation exercise system designed to increase bone density in spinal cord injured individuals," *IEEE Trans. Rehab. Eng.*, vol 1, pp. 213-219, 1993

[3] I. Arvidsson, "Prevention of quadriceps wasting after immobilization: an evaluation of :the effect of electrical stimuation," *Orthopaedics*, vol 9, p. 1519, 1986.

[4] R.W. Fields, "Electromyographically triggered electric muscle stimulation for chronic hemiplegia," *Arch. Phys. Med. Rehabil.*, vol 68, pp. 407-413, 1983.

[5] R. S. Gotlin, S. Hershkowitz, P. M. Juris, E. G. Gonzalez, N. Scott, J. N. Insall, "Electrical stimulation effect on extensor lag and length of hospital stay after total knee arthroplasty," *Arch. Phys. Med. Rehabil.*, vol 75, pp. 957-959, 1994

[6] M.W. Keith, P.H. Pechham, G.B. Thorpe, K.C. Stroh, B. Smith, J.R. Buckett, K.L. Kilgore, and J.W. Jatch, "Implantable functional neuromuscular stimulation in the tetraplegic hand," *J. Hand Surg.*, vol 14, pp. 524-530, May 1989.

[7] Y. Handa, T. Handa, Y. Nakatsuchi, Y. Tagi, and N. Hoshimiya, "A Voice-Controlled Functional Electrical Stimulation System for the Paralyzed Hand," Iyodenshi to Seitai Kogaku, vol 23, pp. 292-298, 1985.

[8] D. Rudel, T. Bajd, A. Kralj, and H. Benko," Surface functional electrical stimulation of the hand in quadriplegics," *5th Ann. Confer. Rehail. Eng.*, p. 59, 1982;

[9] M. Wieler, Z. Kenwell, M. Gauthier, M.; et al.. ""Electronic glove" augments tenodesis-grip and hand-opening in people with quadriplegia.". *Physiotheapy. Can.*, vol 46, 1994

[10] J.K. Klose, 1994;

[11] E.B. Marsolais, and R. Kobetic R., "Functional walking in paralyzed patients by means of electrical stimulation," Clin. Orthopaedics & Rel. Res., vol 175, pp. 30-36, May 1983.

[12] B.J. Andrews, R.H. Baxendale, R. Barnett, G.F Phillips, T Yamazaki, J.P. Paul, and P.A Freeman, "Hybrid FES orthosis incorporating closed loop control and sensory feedback," vol 10, pp 189-195, Apr. 1987

[13] D Popovic, R. Tomovic, and L. Schwirlich, "Hybrid assistive system- neuroprosthesis for motion," *IEEE Trans. Biomed. Eng.*, vol 36, pp 729-738, 1989

[14] M.R. Solomonow, R. Barratta, D. Shoji, N. D'Ambrosia, W Rightar, R. Walker, and R Beandette, "FES powered reciprocating gait orthosis for paraplegic locomotion," *Proc. Vienna Int. Workshop on Electrical Stimulaiton*, p. 81, 1983

[15] W.W.L. Glenn, and M.L. Phelps, "Diaphragm pacing by electrical stimulaiton of the phrenic nerve," *Neurosurgery*, vol 17, pp. 974-984, 1985

[16] Whiteneck, 1985

[17] G.S. Brindley, C.E. Polkey, D.N Rushton, and L. Cardozo, "Sacral anterior root stimulators for bladder control in paraplegia: the first 50 cases," *J. Neurol. Neurosurg Psychiatry*, vol 49, pp. 1104-1114, 1986;

[18] G.S. Brindley, and D.N. Rushton, "Long-term follow-up of patients with sacral anterior root stimulator implants," *Paraplegia*, vol 28, pp. 469-475, 1990.

[19] N.R. Binnie, A.N. Smith, G.H. Creasey, and P. Edmond, "Constipation associated with chronic spinal cord injury: the effect of pelvic parasympathetic stimulaiton by the Brindley stimulator," *Paraplegia*, vol 29, pp. 463-469, Sept. 1991.

[20] A.S. Haleem, F. Boehm, A.D. Legatt, A. Kantrowitz, B. Stone, and A. Melman, "Sacral root stimulation for controlled micturition: prevention of detrusor-external sphincter dyssynergia by intraoperative identification and selective section of sacral nerve branches," J. of Urology, vol 149, pp.1607-12, Jun. 1993.

[21] A. Stefanovska, S. Rebersek, T. Bajd, and L. Vodovnik, "Effects of electrical stimulation on spasticity," Crit. Rev. Phys. & Rehabil. Med., vol 31, pp. 59-99, 1991.

[22] C.J. Robinson, N.A. Kett, and J.M. Bolam, "Spasticity in spinal cord injured patients: 2. Initial measures and long-term effects of surface electrical stimulation," *Arch. Phys. Med. Rehabil.*, vol 69, pp. 862-868, 1988

[23] R.L. Waters, D.R. McNeal, and J. Perry, "Experimental Correction of Footdrop by Electrical Stimulation of the Peroneal Nerve," J. Bone & Joint Surg., vol. 57, pp1047-1054, Dec. 1975.

[24] P. Strojnik, R. Acimovic, e. Vavken, V. Simic, and U. Stanic, "Treatment of drop foot using and implantable peroneal underknee stimulator," *Scand. J. Rehab. Med.*, vol 19, pp. 37-43, 1987.

[25] G.E. Loeb, C.J. Zamin, J.H. Schulman, P.R. Troyk, "Injectable microstimulator for functional electrical stimulation," *Med. & Biol. Eng. & Comput.*, vol 29, pp. 13-19, November 1991.

[26] D.L. Guyton, F.T. Hambrecht, "Theory and design of capacitor electrodes for chronic stimulation," *Med. & Biol. Eng. & Comput.*, vol 12, pp. 613-619, 1974

[27] L.S. Robblee, J.L. Lefko, S.B. Brummer, "Activated Ir: An electrode suitable for reversible charge injection in saline solution," *J. Electrochem. Soc.*, vol 130, pp. 731-733, 1983

[28] D.A.J. Rand, and J. Turner, "Cyclic voltammetric studies on iridium electrodes in sulphuric acid solutions. Nature of oxygen layer and metal dissolution," *Electroanal. Chem. Interfac. Electrochem.*, vol 55, pp. 375-381, 1974

[29] E. Gruys E, J.M. Schakenraad, L.K. Kruit, and J.M. Bolscher , "Biocompatibility of glass-encapsulated electronic chips (transponders) used for the identification of pigs," Veterinary Rec. vol 133, pp. 385-388, Oct. 1993.

[30] Standard Method for Analyzing stress in glass, American Society for Testing and Materials, from Annual Book of ASTM, 1978.

[31] P.R. Troyk, M.A. Schwan, "Class E driver for transcutaneous power and data link for implanted electronic devices," *Med. & Biol. Eng. & Comput.*, vol 30, pp. 69-75, January 1992.

[32] P.R. Troyk, M.A. Schwan, "Closed-loop class E transcutaneous power and data link for microimplants," *IEEE Trans. Biomed. Eng.*, vol 39, pp. 589-99, June 1992

[33] Z.P. Fang, and J.T. Mortimer, "Alternate excitation of large and small axons with different stimulation waveforms: an application to muscle activation," *Med. & Biol. Eng. & Comput.*, vol 29, pp. 543-547, Sept. 1991

[34] T.Cameron, G.E.Loeb, F.J.R.Richmond, R.A.Peck, J.H.Schulman, P.Strojnik, and P.Troyk, "Micromodular Electronic Devices to Activate Paralyzed Muscles and Limbs" Proceedings of the IEEE EMBS

[35] J.H. Schulman, G.E. Loeb, and P.R. Troyk, "Microstimulator for functional neuromuscular control," Quarterly Progress Report #8, Contract # N01-NS-9-2327, Jan. 1991

[36] G. Barolat, "Experience with 509 plate electrodes implanted epiduarally form C1 to L1," Stereotactic & Functional Neurosurgery, vol 61, pp. 50-79, 1993

[37] J.R. Buckett, P.H. Peckham, G.B. Thrope, S.D. Braswell, and M.W. Keith, "A flexible, portable system for neuromuscular stimulation in the paralyzed upper extremity," IEEE Trans. Biomed. Eng., vol 35, pp. 897-904, Nov. 1988.

[38] P. Stojnik, P. Meadows, J.H. Schulman, and D. Whitmoyer, "Modification of a cochlear stimulaiton system for FES applications," Basic and App. Myology, vol 4, pp. 129-140, 1994.

[39] N. Donaldson, "A new mulitplexed stimulator for FNS," *In: Advances in external control of human extremities X.* Belgrade, Yugoslav comittee for ETAN, pp. 41-50, 1987.

[40] Y. Handa, T. Handa, M. Ichie, H. Murakami, N. Hosimiya, S. Ishikawa, and K. Ohkubo, "Functional electrical stimulation (FES) systems for restoration of motor function of paralyzed muscles - versatile systems and a portable system," Frontiers Med. Biol. Engng., vol 4, pp. 241-255, 1992.

[41] R.W. Booth, and E.W. Gould, "Effects of training and disuse on connective tissue," *Exercise Sport Sci. Rev.*, vol 3, pp. 83-112, 1975.

[42] R.W. Booth, and P.D. Gollnick, "Effects of disuse on the structure and function of skeletal muscle," *Med. Sci. Sports Exercise*, vol 15, pp. 415-420, 1983.

[43] M.R. Gossmann, S.J. Rose, S.A. Sahrmann, and C.R. Kathol, "Comparison of sarcomere changes in the plantaris and soleus muscles in the rabbit following immobilization," *Phys. Ther.*, vol 65, p. 698, 1985.

[44] M.S. Nash, A.M. Kumar, J.R. Hughes, J.B. Fernandez, A.E. Marcillo, K.J. Klose, and M. Kumar, "Acute serotonergic and cortisol responses of quadriplegics to electrically-stimulated cycling exercise," *J. Amer. Para. Soc.*, vol 15, p. 75, April 1992.

[45] T. N. Hangartner, M.M. Rodgers, R.M. Glaser, "Tibial bone density loss in spinal cord injured patients: Effects of FES exercise," *J. Rehabil. Res. & Develop.*, vol 31, pp. 50-61, 1994.

[46] G.M. Yarkony, E.J. Roth, G.R. Cybulski, and R.J. Jaeger, "Neuromuscular stimulation in spinal cord injury II: Prevention of secondary complications," Arch. Phys. Med. & Rehabil., vol 73, pp. 195-200, Feb. 1992.

[47] J.M. Campbell, and P.M. Meadows, "Therapeutic FES: From rehabilitation to neural prosthetics," *Assist. Technol.*, vol 4, pp. 4-18, 1992.

[48] L.L. Baker, and K. Parker, "Neuromuscular electrical stimulation of the muscles surrounding the shoulder," Phys. Therap., vol 66, pp. 1930-1937, Dec. 1986.

[49] P. D. Faghri, M.M. Rodgers, R.M. Glaser, J.G. Bors, C. Ho, and P. Akuthota, "The effects of functional electrical stimulation on shoulder subluxation, arm function recovery, and shoulder pain in hemiplegic stroke patients," *Arch. Phys. Med. Rehabil.*, vol 75, pp. 73-79, Jan. 1994.

Suppliers

1. Kimbel borosilicate glass type N51A, formed by Friedrich & Dimmock, Wheaton Ave., Milliville, NJ 08332, (609)825-0305
2. AVX Tantalum Corp., 69 Landry St., Biddeford, ME 04005 (207)282-5111
3. vendor to be selected by A.E. Mann Foundation
4. Cermaic Magnetics Inc., 16 Law Dr., Fairfield, NJ 07004 (201)227-4222
5. Engelhard Industries, 100 Engelhard Dr., Aurora, Ont. K4G 3N1 (416)727-3191
6. Glenmark Manufacturing Inc. 970 Woodlands Park, Unit B, Vernon Hills, Ilinois

Part Name	Abbreviation	Specification
Glass Capillary	Cap	N51A borosilicate, 0.079"OD ± 0.[illegible]
Glass Bead	Bd	0.015"ID, 0.065"OD, 0.04"thickness
Glass Washer	Ws	0.015"ID, 0.065"OD, 0.01"thickness
Ferrite Top	Fe-T	0.25" radius, 0.16" core length
Ferrite Bottom	Fe-B	0.25" radius, 0.16" core length
Tantalum Sug	Ta slug	0.046" diameter, 0.039" thickness
Iridium Ball	Ir ball	0.065" diameter
Gold Plated Metal Shim	Shim	0.18" length, 0.042" width, 0.004" height
Gold Plated Wire Feedthrough	Au-W	0.008" OD, 0.2" long
Integrated Circuit Chip	IC chip	3 micron, double poly, c-mos, p-well
Diode	D	THD 9064
Copper Coil	Cu coil	25 μm diameter

Figure 1

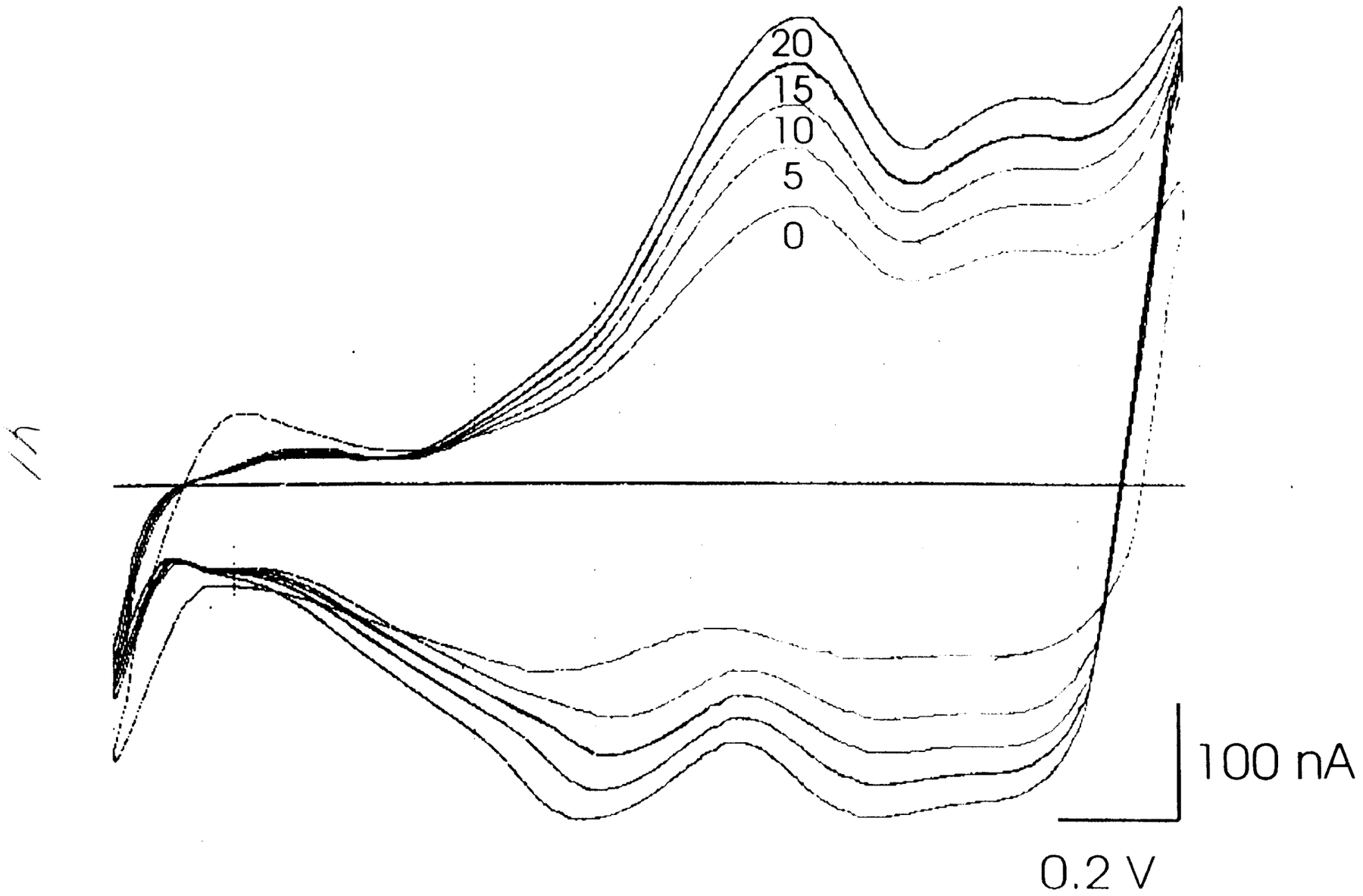

Figure 2

High Stress Seal

Low Stress Seal

A=18° cw

A=4°cw

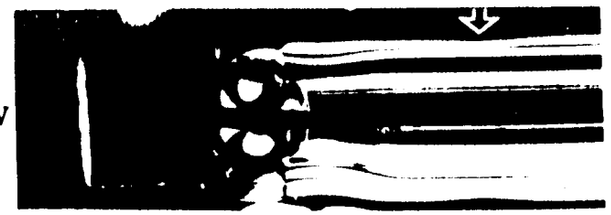

A=18° ccw

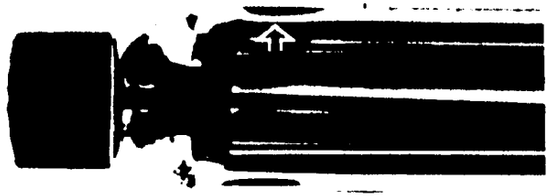

A=4° ccw

S = 6607 psi

S = 1468 psi

$$S = \frac{K \times \lambda \times \frac{A}{180^\circ}}{B \times \sqrt{WD}}$$

S = bending stress (psi)

K = geometric factor for cylindrical tube (1.5)

λ = perceived wavelength of white light (567nm)

A = mean angular rotation (180° = full wave)

B = stress optical coefficient of type 7800 glass (0.235 nm / cm / psi)

D = outside diameter of tube (0.2cm)

W = wall thickness (0.015cm)

Figure 3

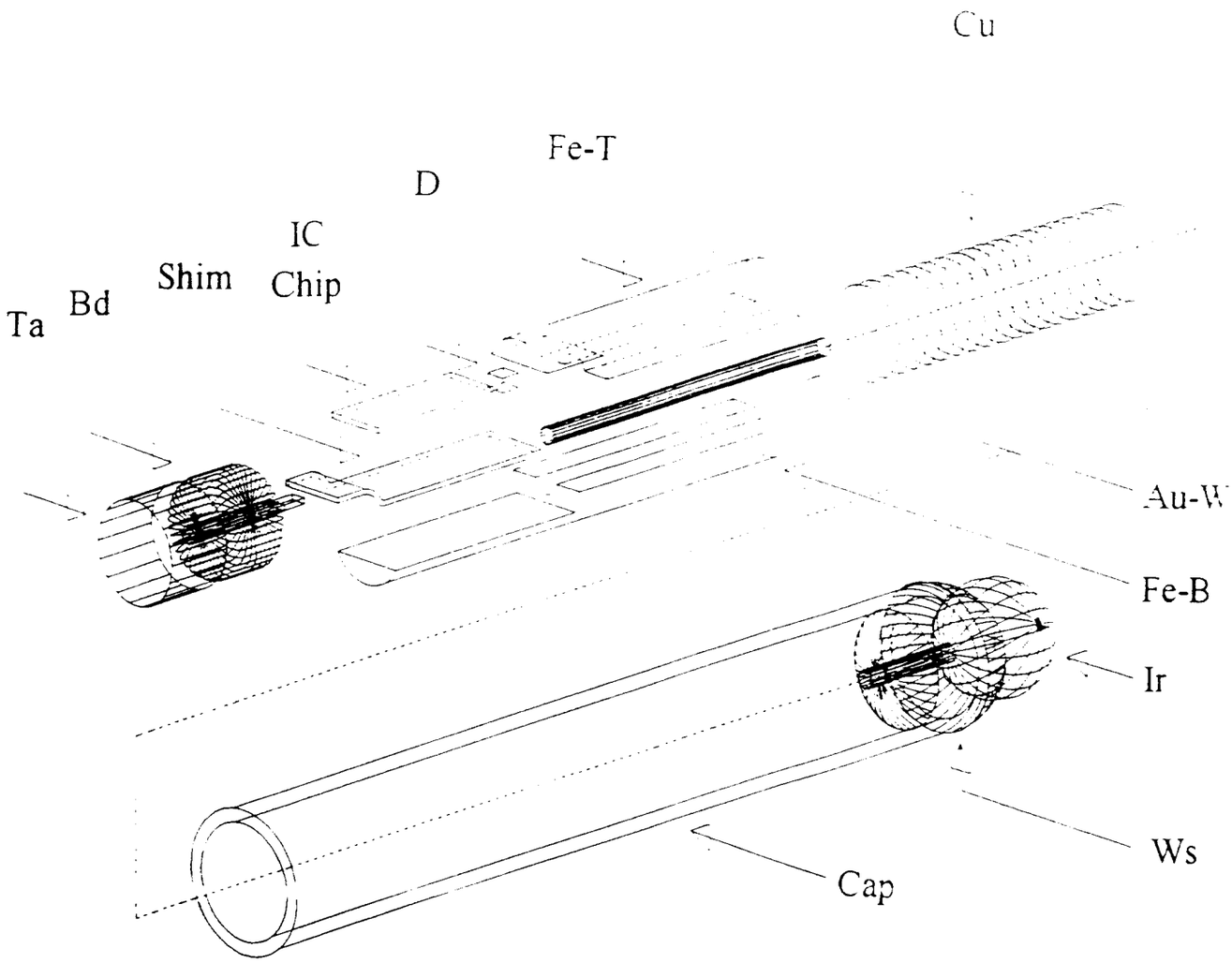

Figure 4

4/

μ Stimulator Fabrication Sequence

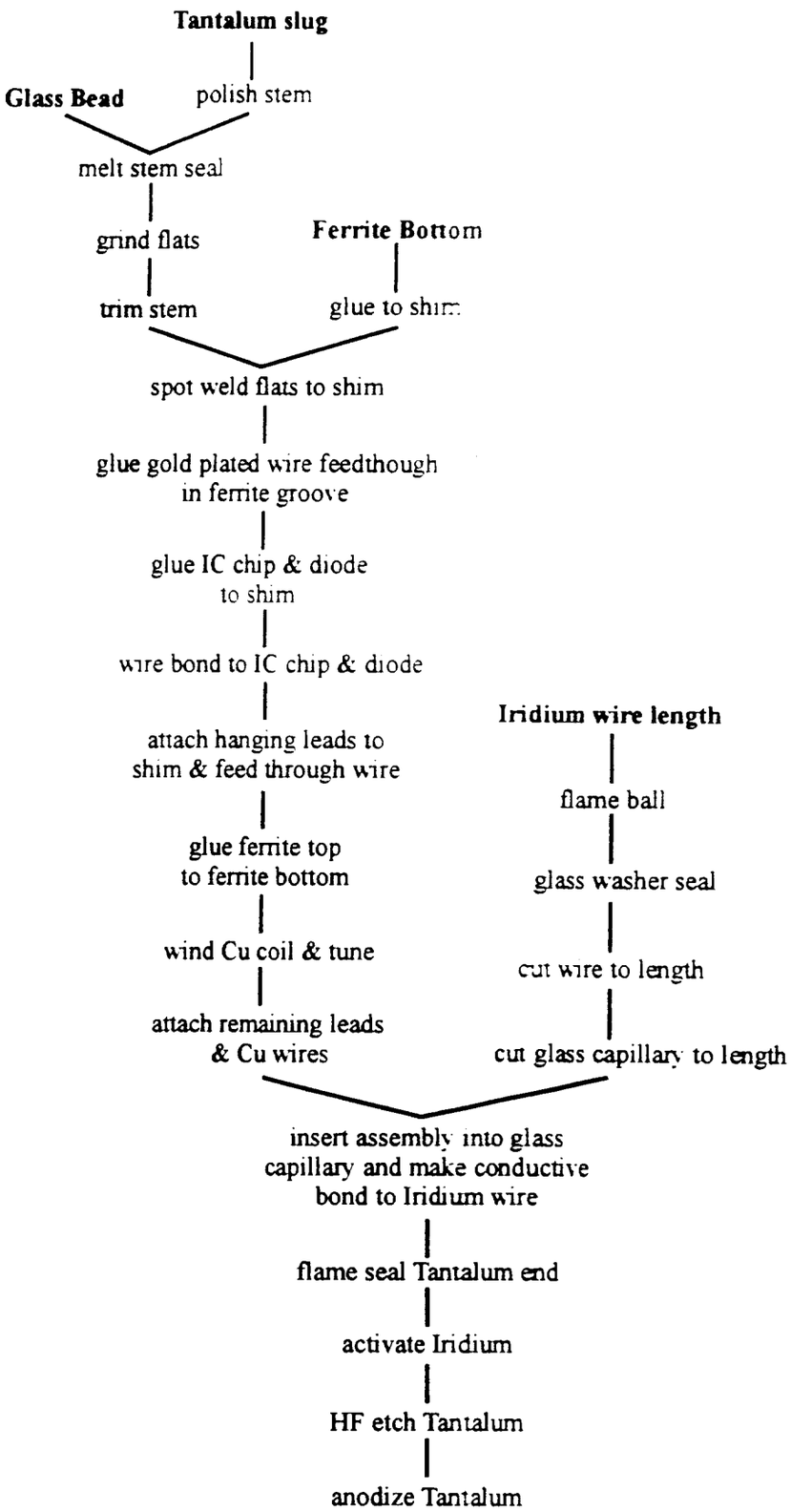

Figure 5

44

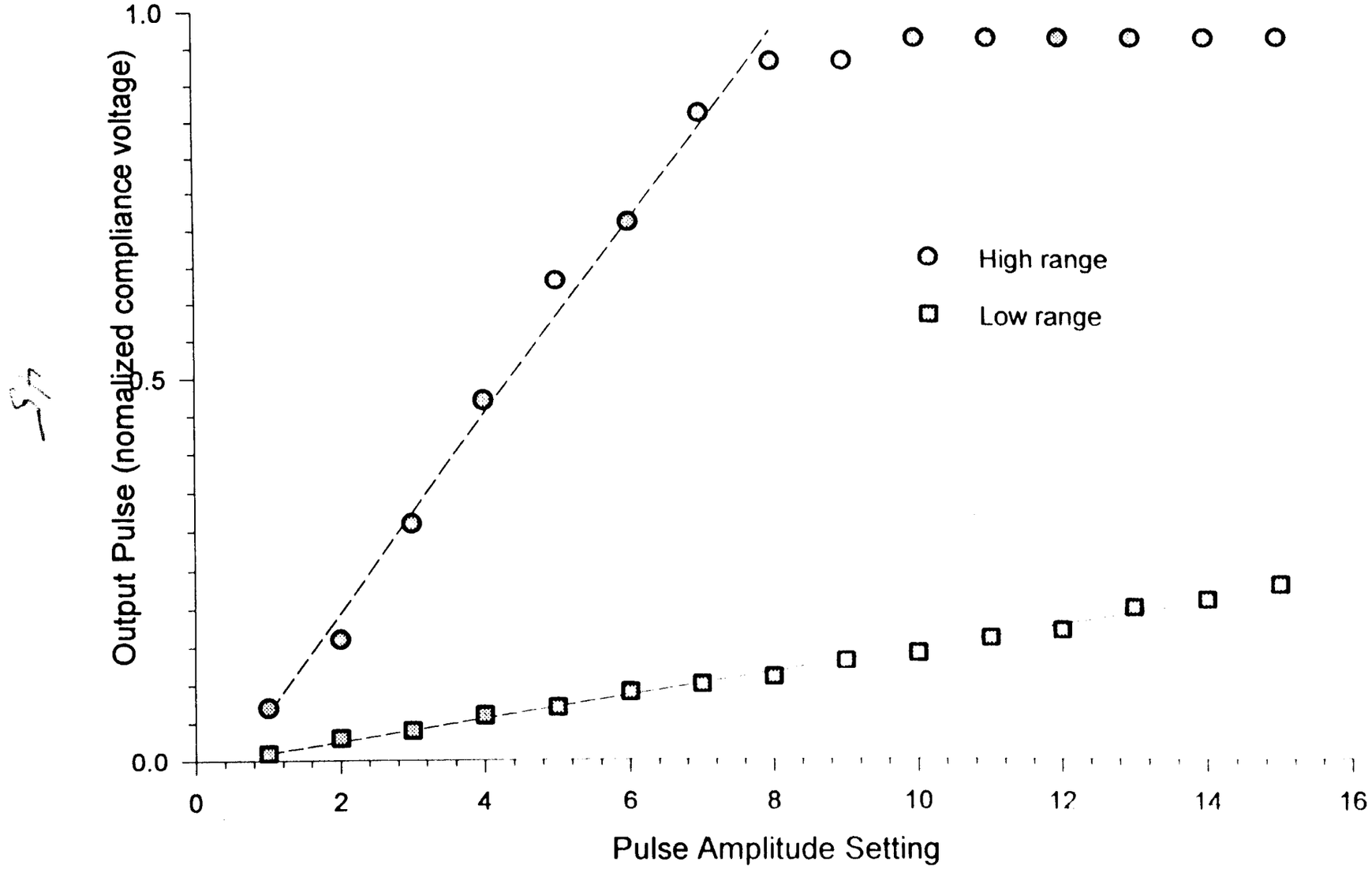
1.0
0.5
0.0
Output Pulse (nomalized compliance voltage)
High range
Low range
0
2
4
6
8
10
12
14
16
Pulse Amplitude Setting

Figure 6

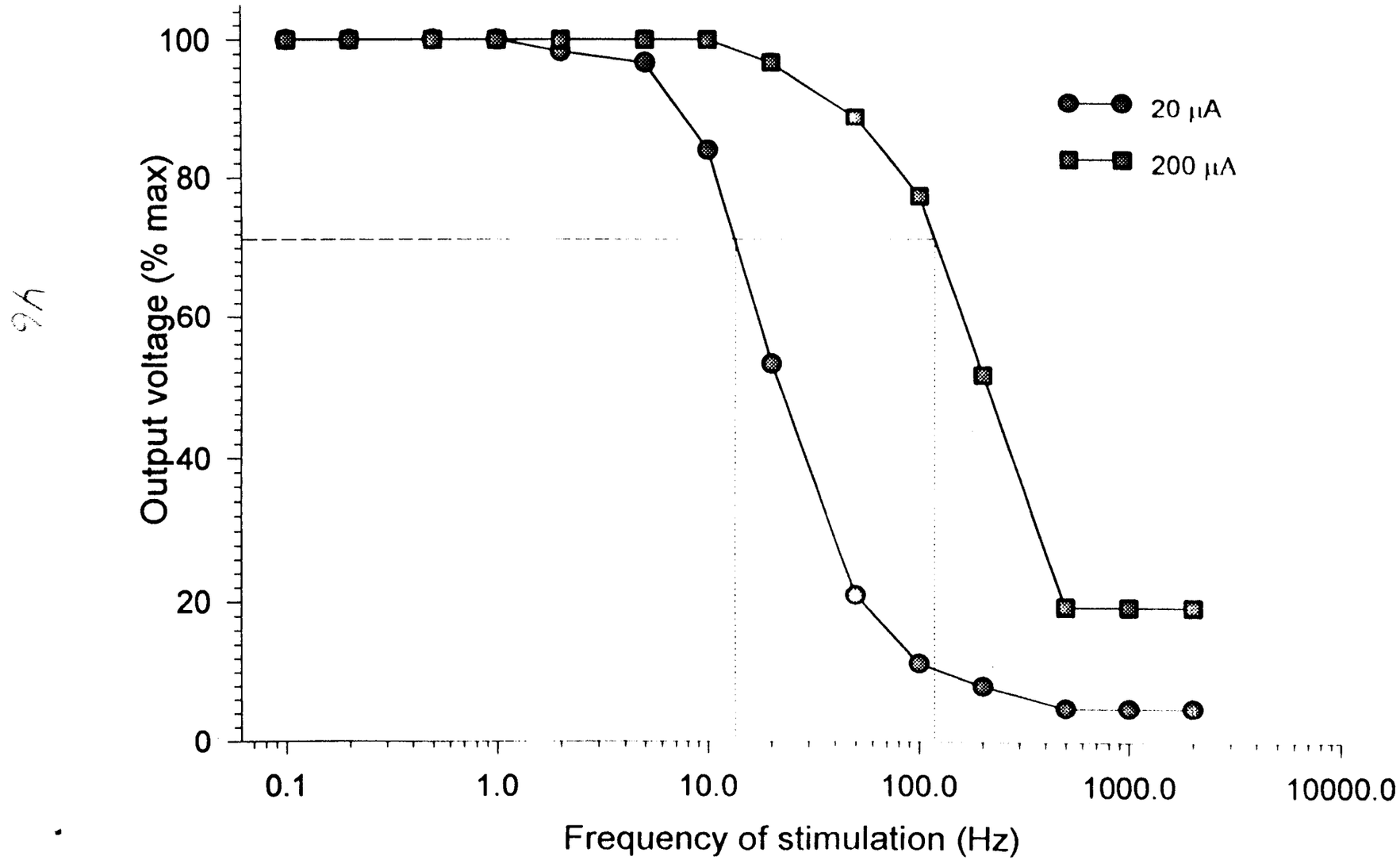
100
80
60
40
20
0
Output voltage (% max)
0.1
1.0
10.0
100.0
1000.0
10000.0
Frequency of stimulation (Hz)
20 µA
200 µA

Figure 7

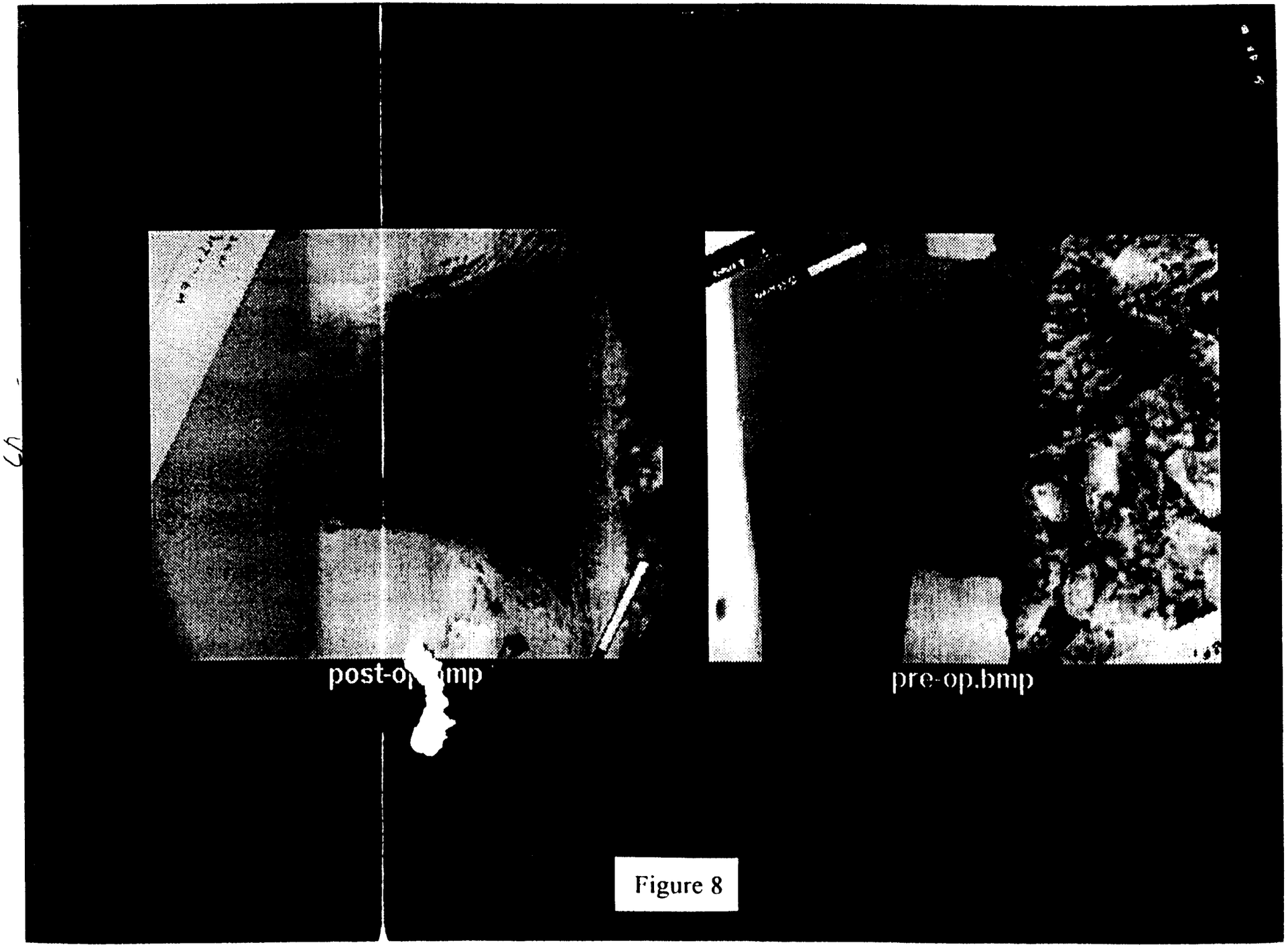

Figure 8

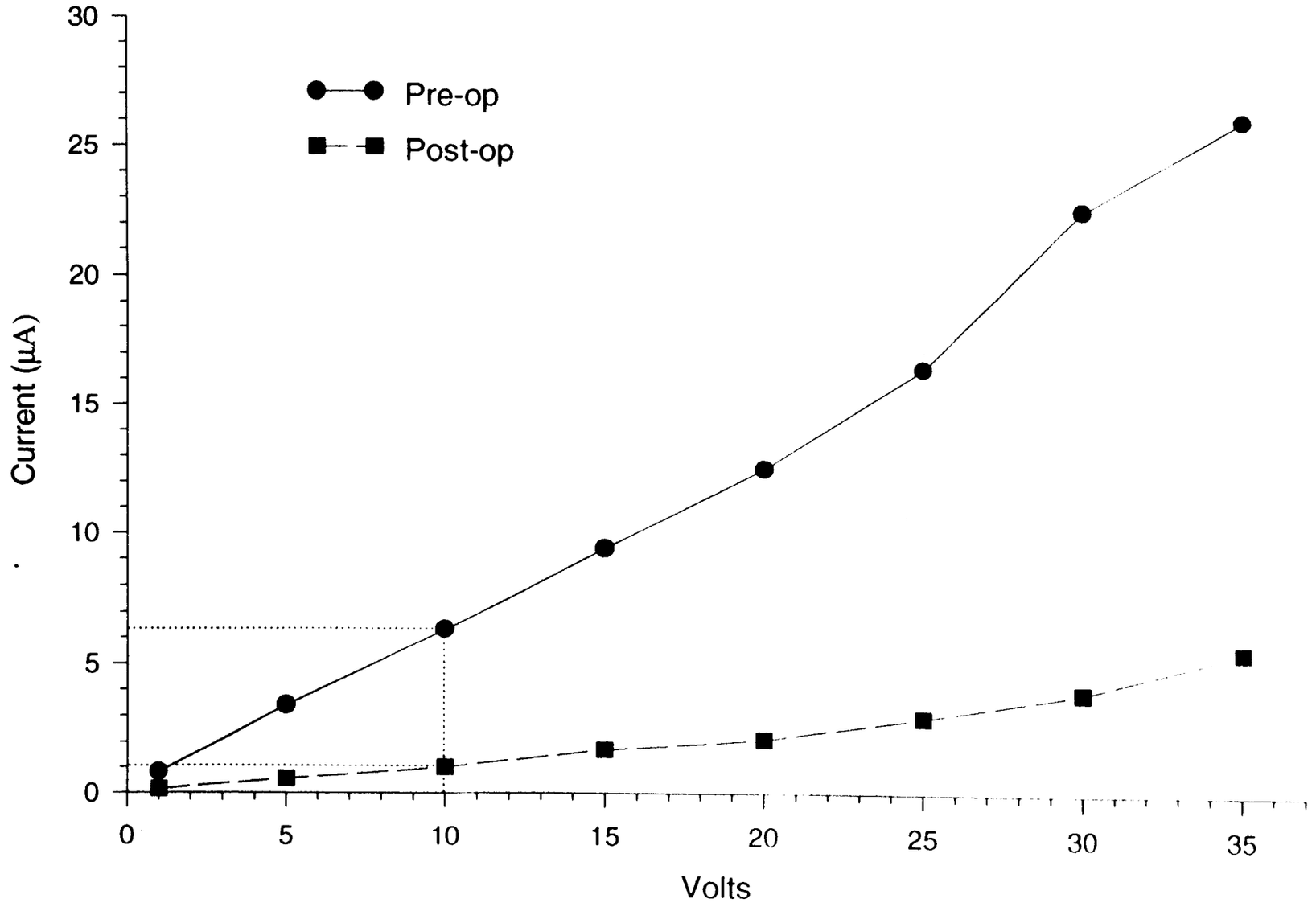

Figure 9